Heliyon 10 (2024) e31311

Contents lists available at ScienceDirect

Heliyon

journal homepage: www.cell.com/heliyon

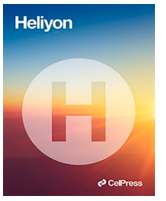

Research article

Identification of potential tissue-specific biomarkers involved in pig fat deposition through integrated bioinformatics analysis and machine learning

Yongli Yang [1], Mingli Li [1], Yixuan Zhu, Xiaoyi Wang, Qiang Chen, Shaoxiong Lu [*]

Faculty of Animal Science and Technology, Yunnan Agricultural University, Kunming, 650201, Yunnan, China

ARTICLE INFO

Keywords:
Subcutaneous adipose
Intramuscular fat
Bioinformatics analysis
Machine learning
Biomarkers

ABSTRACT

Backfat thickness (BT) and intramuscular fat (IMF) content are closely appertained to meat production and quality in pig production. Deposition in subcutaneous adipose (SA) and IMF concerns different genes and regulatory mechanisms. And larger studies with rigorous design should be carried to explore the molecular regulation of fat deposition in different tissues. The purpose of this study is to gain a better understanding of the molecular mechanisms underlying differences in fat deposition among different tissues and identify tissue-specific genes involved in regulating fat deposition. The SA-associated datasets (GSE122349 and GSE145956) and IMF-associated datasets (GSE165613 and GSE207279) were downloaded from the Gene Expression Omnibus (GEO) as the BT and IMF group, respectively. Subsequently, the Robust Rank Aggregation (RRA) algorithm identified 27 down- and 29 up-regulated differentially expressed genes (DEGs) in the BT group. Based on bioinformatics and three machine learning algorithms, four SA deposition-related potential biomarkers, namely *ACLY*, *FASN*, *ME1*, and *ARVCF* were selected. *FASN* was evaluated as the most valuable biomarker for the SA mechanism. The 18 down- and 34 up-regulated DEGs in the IMF group were identified, and *ACTA2* and *HMGCL* were screened as the IMF deposition-related candidate core genes, especially the *ACTA2* may play the critical role in IMF deposition regulation. Moreover, based on the constructed ceRNA network, we postulated that the role of predicted ceRNA interaction network of XIST, NEAT1/miR-15a-5p, miR-16-5p, miR-424-5p, miR-497-5p/*FASN* were vital in the SA metabolism, XIST, NEAT1/miR-27a/b-3p, 181a/c-5p/*ACTA2* might contribute to the regulation to IMF metabolism, which all gave suggestions in molecular mechanism for regulation of fat deposition. These findings may facilitate advancements in porcine quality at the genetic and molecular levels and assist with human obesity-associated diseases.

1. Introduction

Fat deposition and distribution are closely related to meat quality and flavor. Backfat thickness (BT) and intramuscular fat (IMF) content are two vital traits related to fat deposition. IMF content affects meat quality traits such as pH, meat color, tenderness and flavor, while BT is also associated with pork quality traits and economic value [1]. A decrease in BT is beneficial for an increase in lean

* Corresponding author.
E-mail address: shxlu_ynau@163.com (S. Lu).
[1] these authors contributed equally to this work.

https://doi.org/10.1016/j.heliyon.2024.e31311
Received 27 January 2024; Received in revised form 10 May 2024; Accepted 14 May 2024
Available online 15 May 2024

Table 1
Details of all datasets.

Group	GEO	Platform	Tissue (pig)	Index	Breeds	Samples (number)			Attribution
						low group	high group	Total	
BT group	GSE122349	GPL21186	Dorsal subcutaneous fat	Backfat thickness	Pulawska pigs (low/high-BT)	8	8	16	Test
	GSE145956	GPL11429	Dorsal subcutaneous fat	Backfat thickness	Bísaro pigs(low-BT), Alentejano pigs(high-BT)	4	4	8	Test
	GSE61271	GPL19176	Subcutaneous fat	Obesity Index	F2 population of Duroc × Göttingen minipig intercross (lean and obesity pigs)	12	12	24	Validation
IMF group	GSE165613	GPL22475	longissimus dorsi muscle	Phenotypes (BT,IMF)	Nanyang black pigs (low/high-fat deposition group)	3	3	6	Test
	GSE207279	GPL22475	longissimus dorsi muscle	Intramuscular fat content	Laiwu pigs(low/high-IMF)	3	3	6	Test
	GSE180840	GPL22918	longissimus dorsi muscle	–	Luchuan pigs (obese pig), Duroc boars (lean pig)	3	3	6	Validation

percentage, and an increase in IMF content contributes to palatability and meat quality [2]. Therefore, how to increase IMF content while reducing subcutaneous adipose (SA) deposition is a key issue for meat quality regulation in pig breeding. Moreover, pigs and humans share a high degree of homology in genome sequence and chromosome structure, as well as greater similarities in physiological characteristics. Pigs are often used as an optimal biomedical model for the study of obesity and metabolic-related diseases [3,4]. Through relevant research, we may provide a new theoretical basis for health problems, and also make pigs more medically useful.

Fat deposition is a dynamic process that includes the operations of fat synthesis, decomposition, and transportation [5]. The increasing number of studies has revealed that the relative development of fat deposition differs between SA and IMF. It was found that subcutaneous adipocytes were stronger than intramuscular adipocytes in terms of fat differentiation and deposition by comparing primary differentiated adipocytes of SA and IMF in pigs [6]. SA is a major fat type. It is not only a major energy storage organ but also a main endocrine organ. SA plays an essential role in many biological and physiological processes, such as regulating body temperature, energy balance, insulin sensitivity, inflammatory response and cardiovascular response [7]. IMF content has a high impact on various meat quality characteristics. The IMF proliferation rate hinges on the rate of muscle growth. For instance, animals with high muscularity are usually active in glycolysis, which exhibits a reduced development of IMF [8]. IMF has a lower growth rate and lipid content than SA [9]. Furthermore, the subcutaneous and intramuscular adipocytes have specific regulatory mechanism for fat deposition during differentiation owing to different ways of generating lipid droplets [10]. Levels of gene expression in distinct tissues can regulate different biology, indicating that they have different functions, such as *RETREG1* plays an inhibitory role in IMF deposition, but previous studies have identified that it could promote SA deposition [11]. Identifying gene-specific expression patterns in different tissues is useful in the understanding of molecular regulation mechanisms or characteristics assessment for fat deposition and meat quality. However, the intrinsic molecular mechanisms underlying fat deposition in different tissues remain incompletely elucidated, and more research is needed to perform deeper understanding and to explore more tissue-specific regulatory factors.

With the widespread application of high-throughput sequencing technology, numerous key genes and pathways related to SA and IMF are also being discovered [11,12]. In addition, data re-mining using bioinformatics analysis and machine learning algorithms based on public databases has facilitated the screening of potential biomarkers for economic traits in pigs [13,14]. In particular, machine learning algorithms, as a new high-dimensional data analysis method, have shown great promise in predicting the accuracy of trait-related biomarkers [15]. Although a series of experiments have been performed to identify the differences in SA and IMF deposition in pigs, the sample size of each experiment was limited in these studies. Therefore, by merging the related datasets with similar experiments to increase the sample size is an optional method to gain more accuracy and effectiveness for the related studies with bioinformatics analysis and machine learning algorithms.

Therefore, in this study, the SA-associated datasets GSE122349 and GSE145956 and the IMF deposition-associated datasets GSE165613 and GSE207279 were analyzed separately by robust rank aggregation (RRA) method. Moreover, we further explored the potential mechanism of fat deposition of SA and IMF through functional enrichment and protein-protein interaction (PPI) analysis. Then, the potential tissue-specific biomarkers related to fat deposition were screened by bioinformatics and three machine learning methods, and were subjected to real-time PCR analysis for further validation. Moreover, the ceRNA networks was constructed based on the interaction relationship between the predicted miRNAs, IncRNAs, and screened tissue-specific biomarkers to further explore the potential molecular mechanism. The objective of this study was to identify crucial tissue-specific genes associated with fat deposition and investigate their intrinsic mechanisms. Our findings extend the reports of single tissue type studies, and add support to the previous literature investigating associations between fat deposition in different tissues and specific molecular regulation mechanism. Our study may provide more targeted rationale for understanding the regulatory mechanisms of fat deposition in SA and IMF, and develop effective potential tissue-specific biomarkers for optimizing pig fat deposition and treating lipid metabolism-related diseases.

2. Materials and methods

2.1. Gene expression data processing

Six transcriptome-wide gene expression profiles were downloaded from the GEO database (https://www.ncbi.nlm.nih.gov/geo/). The data of GSE122349, GSE145956 and GSE61271 were derived from SA, the pigs were divided into the low- and high-BT groups according to the BT, and GSE61271 was used to validate the expression of the selected genes. GSE165613, GSE207279 and GSE180840 were derived from LDM, the pigs were divided into the low- and high-IMF groups based on the IMF content, and GSE180840 was used as a validation dataset. Details of all datasets are shown in Table 1.

2.2. Datasets analysis

The differentially expressed genes (DEGs) between the low- and high-BT group and the low- and high-IMF group were identified using the "limma" package based on R software (version 4.1.2) [16]. The genes with P value < 0.05 and $|\log2\ FC| > 1$ were considered significant DEGs. The expression level and distribution of DEGs were visualized using a heatmap and a volcano plot based on the "heatmap" and "ggplot2" packages (versions 3.3.6), respectively.

2.3. RRA analysis

The robust rank aggregation (RRA) method, which takes the intersection of multiple sequenced gene sets to screen out the genes that exhibit differences and rank high in each dataset, was utilized to integrate and analyze SA deposition-related datasets

(GSE122349, GSE145956) and IMF deposition-related datasets (GSE165613, GSE207279) to obtain the common DEGs based on "RRA" package [17]. Genes with P value < 0.05 and $|\log2\ FC| > 0.5$ in the ranking list were considered as robust DEGs.

2.4. Merging of the datasets

The SA deposition-related gene expression datasets were merged into a new dataset as BT group, which was corrected for batch effects via the "sva" R package [18]. The IMF deposition-related gene expression datasets were combined as the IMF group for subsequent studies.

2.5. Functional enrichment analysis

The gene ontology (GO) analysis was performed using the R "clusterProfiler" package (version 4.4.4) in the Bioconductor project (version 3.15) to conduct large-scale functional enrichment, including BP, MF and CC analyses. The Kyoto Encyclopedia of Genes and Genomes (KEGG) pathway enrichment analysis was performed by the KOBAS (http://kobas.cbi.pku.edu.cn/). Functional terms with P value < 0.05 were considered to significantly change, and the top 10 GO functional terms were visualized using the ggplot2 package, and the top 10 KEGG terms were visualized using the Sangerbox online tool (http://sangerbox.com/). To further investigate the biological function of individual genes, Gene set enrichment analysis (GSEA) was performed via the "clusterProfiler" package and "GSEABase" (version 1.58.0) R software, and enrichment terms with statistically significant differences were visualized using the "enrichplot" package (version 1.16.1).

2.6. PPI network construction and hub genes identification

The interactive relationships among the protein-coding DEGs were elucidated though the STRING database (https://cn.string-db.org/) by constructing the PPI network and visualized by Cytoscape software (version 3.9.1). Hub genes were identified using the Maximal Clique Centrality (MCC) method in the Cytoscape plugin cytoHubba [19], and the top 10 genes with the highest score were selected as hub genes. The correlation of the hub genes was then analyzed and visualized by the Pearson analysis through the online website Sangerbox.

2.7. Screening of potential biomarkers based on machine learning algorithms

Three machine learning algorithms, including least absolute shrinkage and selection operator (LASSO) [20], support vector machine-recursive feature elimination (SVM-REF) [21] and Random Forest machine learning algorithm [22], were used to screen for biomarkers among the top 10 hub genes identified in the PPI network. First, the "glmnet" R package was utilized for proceeding with the analysis of the LASSO [23]. Then, the "e1071" R package was utilized for performing the SVM-REF [24]. Meanwhile, the "randomForest" R package was utilized for proceeding with the Random Forest machine learning [25], and the five most significant genes were retained for the following analysis. The overlapping genes produced by the three machine learning algorithms were considered as potential biomarkers. GSEA of the potential biomarkers was then done to further explore their possible biological functions.

2.8. Validation and predictive evaluation of the potential biomarkers

The predictive effect of the potential biomarkers was further validated in the SA deposition-related dataset GSE61271 and IMF deposition-related dataset GSE180840. Firstly, the unpaired t-test method was used for analyzing the expression levels of potential biomarkers in the validation dataset, with a P value < 0.05 considered significant. Subsequently, ROC analysis was performed in the validation sets, and the area under curves (AUC) values were calculated using GraphPad Prism 8 to evaluate whether potential biomarkers had good distinguishing performance. The biomarker with an AUC $>$ 0.7 was considered a potential biomarker.

2.9. Construction of potential TF-biomarker regulatory network

TFs of potential biomarkers were predicted using the online database UCSC and JASPAR 2022(https://genome.ucsc.edu/) (the screening condition of minimum score: 500), Human TFDB 3.0 (http://bioinfo.life.hust.edu.cn/HumanTFDB#!/). The co-expression networks of the predicted TFs and potential biomarkers were then visualized through the Cytoscape software (version 3.9.1).

2.10. Construction of ceRNA network

The prediction of lncRNAs and miRNAs targeting the hub genes were performed to established the lncRNA-miRNA-mRNA ceRNA network, and the ceRNA network was constructed based on the ceRNA hypothesis, whereby LncRNAs act as miRNA sponges to indirectly modulate mRNA expression by directly binding to miRNAs [26]. To start, the miRNAs for the hub genes were predicted using the databases, miRanda [27], TargetScan [28]. Then, the co-expression of miRNA and lncRNA was researched according to these predicted miRNAs. Finally, the ceRNA network was constructed based on above co-expression results, and visualized using the Cytoscape software.

2.11. Animals and tissue collection

Two types of pig breeds, Saba (fat type) and Large White (lean type) were used to validate the potential biomarkers, which Saba pig was an indigenous breed in Yunnan, China. Due to the diverse grouping of experimental animals in the dataset we used, including extremely different BT and IMF comparisons within the same breeds, as well as comparisons between different breeds, the pigs used for validation were grouped in two ways. For the validation of SA deposition-related biomarkers, six Saba pigs (three with extremely high and three with extremely low BT), three Saba pigs (fat pig with high BT) and three Large White pigs (lean pig with low BT) were used; six Saba pigs (three with extremely high and three with extremely low IMF content), three Saba pigs (fat pig with high IMF) and three Large White pigs (lean pig with low IMF) were used for the validation of biomarkers related to IMF deposition. All of the pigs were raised to 100–110 kg under identical environmental and feeding conditions, and then slaughtered. The dorsal SA and LDM samples were collected from the carcasses at slaughter, snap frozen in liquid nitrogen and maintained at −80 °C until total RNA extraction, some LDM were stored at −20 °C for determination of IMF content by the Soxhlet extraction method. BT was measured based on the average of three measurements including BT over the thickest part of the shoulder, at the last rib and at the sacrum part of the spine using vernier calipers. All animal procedures were performed according to the principles of the Laboratory Animal Care and Use Guidelines issued by the Animal Research Committee of Yunnan Agricultural University, the experimental protocol was approved by the Animal Ethics Committee of Yunnan Agricultural University (approval ID: 202310003).

2.12. RNA extraction and qRT-PCR

Total RNA was extracted from dorsal SA and LDM samples using RNA sample total Extraction Kit (Tiangen, Beijing, China). Reverse transcription was performed using PrimeScript™ RT reagent Kit with gDNA Eraser (Takara, Dalian, China) according to the manufacturer's instructions. qRT-PCR assay was performed using TB Green® Premix Ex Taq™ II (Tli RNaseH Plus) (Takara, Dalian, China) on a qRT-PCR system (Mx3000P, Agilent Technologies). The gene-specific qRT-PCR primers were listed in Supplementary Table S1. Each experiment was performed in triplicates, and the relative expression of mRNA was calculated through the $2^{-\Delta\Delta Ct}$ method, GAPDH was used as the internal control for normalization. Relative mRNA expression levels were compared by unpaired *t*-test using SAS software (version 9.2), and $P < 0.05$ and $P < 0.01$ were considered significant and extremely significant, respectively.

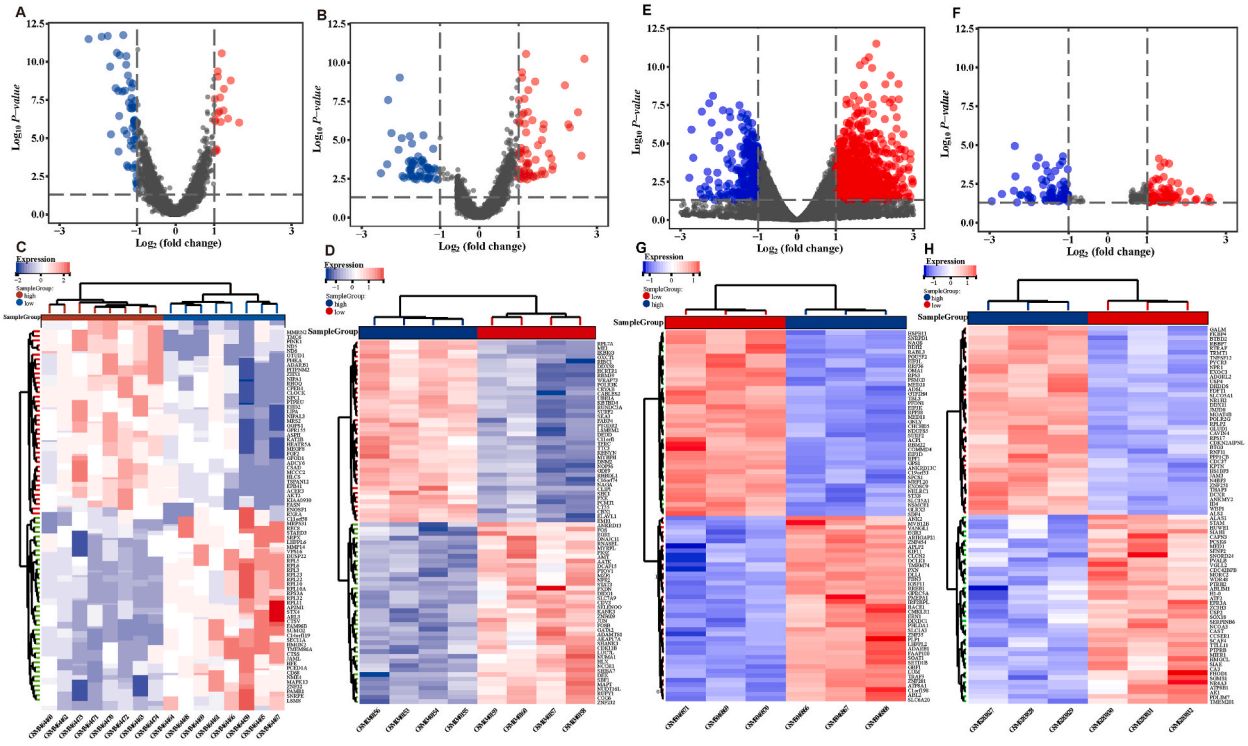

Fig. 1. Distribution and volcanogram of DEGs of the test datasets. (A, C) GSE122349. (B, D) GSE145956. (E, G) GSE165613. (F, H) GSE207279.

3. Results

3.1. DEGs identification

The GSE122349 dataset contained 552 DEGs, including 149 up- and 403 down-regulated genes (Supplementary Table S2). The GSE145956 dataset contained 284 DEGs, including 131 up- and 153 down-regulated genes (Supplementary Table S3). The GSE165613 dataset contained 1190 DEGs, including 936 up- and 254 down-regulated genes (Supplementary Table S4). The GSE207279 dataset contained 132 DEGs, including 69 up- and 63 down-regulated genes (Supplementary Table S5). The DEGs of the SA deposition-related datasets GSE122349 and GSE145956 were shown in Fig. 1A and B, and the heatmap of the DEGs were shown in Fig. 1C and D. The DEGs of the IMF deposition-related datasets GSE165613 and GSE207279 were shown in Fig. 1E and F, and the heatmap of the DEGs were shown in Fig. 1G and H.

Then, 56 integrated DEGs in the BT group, comprising 29 up- and 27 down-regulated genes, were identified by the RRA method based on SA deposition-related datasets as shown in Supplementary Table S6, and the top 20 DEGs (10 up- and 10 down-regulated) were shown in Fig. 2A. The 52 integrated DEGs of the IMF group, consisting of 34 up- and 18 down-regulated genes, were identified based on the IMF deposition-related datasets as shown in Supplementary Table S7, and the top 20 DEGs were shown in Fig. 2B. No overlapping DEGs between the BT and the IMF groups were found.

3.2. Functional analysis of DEGs

In the BT group, GO analysis of DEGs from low- and high-BT pigs showed that 52 biological processes (BPs), 7 cellular components (CCs), and 22 molecular functions (MFs) were significantly enriched ($P < 0.05$) (Supplementary Table S8). KEGG enrichment analysis revealed 12 significantly enriched pathways ($P < 0.05$) (Supplementary Table S9). The top 10 GO and KEGG terms with the smallest P values are shown in Fig. 3A and C. GO functional enrichment analysis revealed that DEGs were mainly involved in carboxylic acid metabolic/biosynthetic process, oxoacid metabolic process, organic acid metabolic/biosynthetic process, fatty acid biosynthetic process and cardiac muscle contraction. KEGG pathway analysis revealed that DEGs were significantly enriched in metabolic

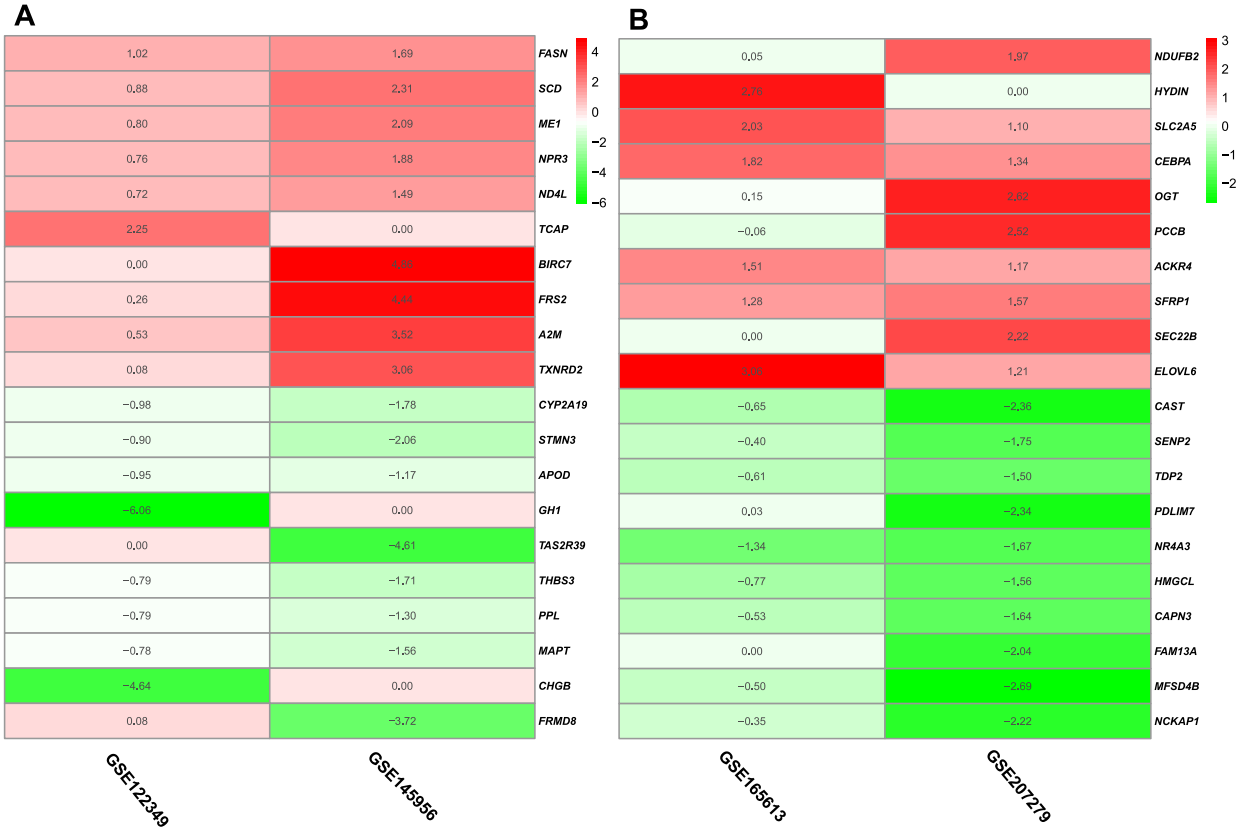

Fig. 2. The heatmap of top 20 DEGs (10 up- and 10 down-regulated) according to RRA method. (A) BT group. (B) IMF group. As the color goes from red to green, indicating the change from up to down regulation. Figure 0 represent genes with no statistical significance in one of the datasets, but it can be reflected in another using the RRA method. (For interpretation of the references to color in this figure legend, the reader is referred to the Web version of this article.)

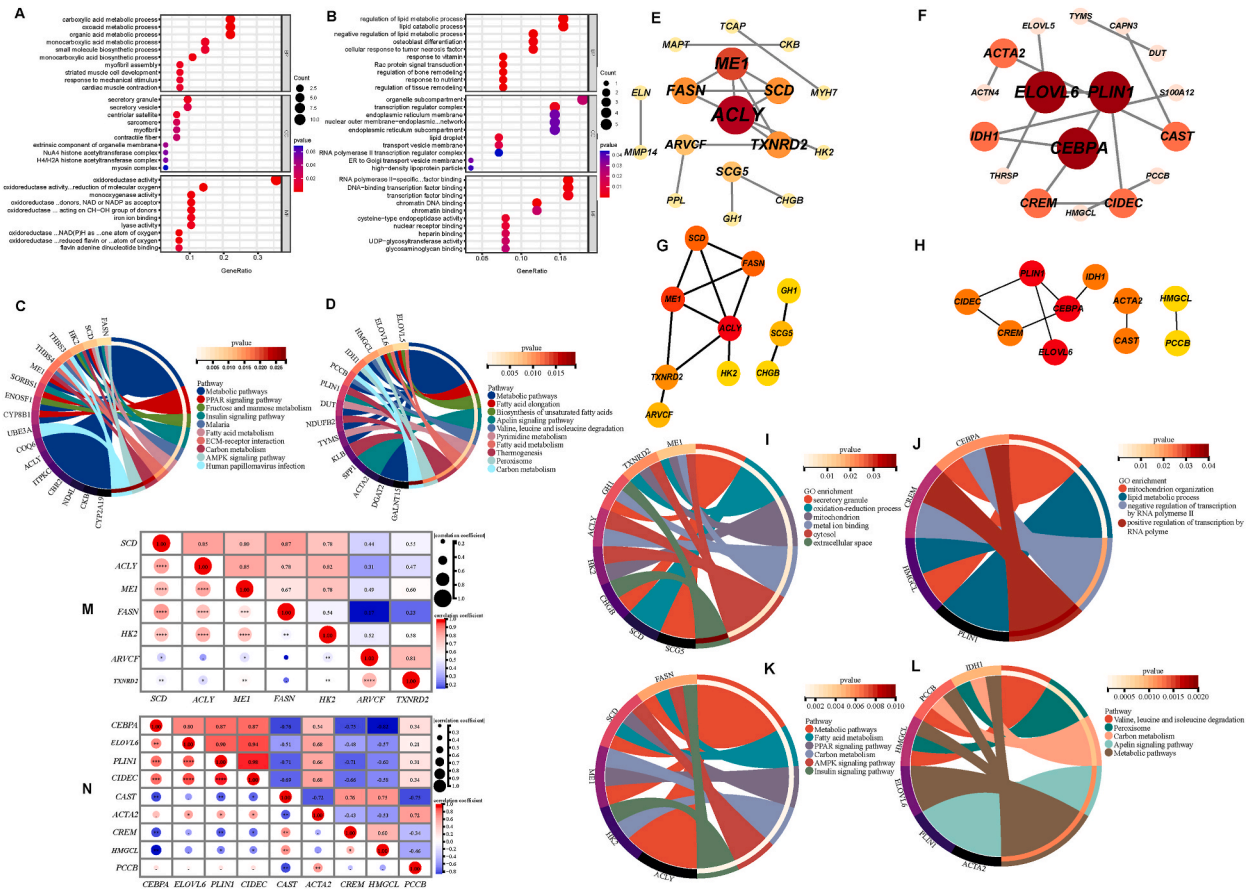

Fig. 3. Hub genes identification and analysis. (A, C) Go and KEGG enrichment of DEGs in BT group. (B, D) Go and KEGG enrichment of DEGs in IMF group. (E) PPT network in BT group. (F) PPT network in IMF group. (G) Ten hub genes from PPT network based on MCC in BT group. (H) Ten hub genes in IMF group. (I, K) Go and KEGG enrichment of hub genes in BT group. (J, L) Go and KEGG enrichment of hub genes in IMF group. (M–N) Correlation matrixes of hub genes in BT group and IMF group.

pathways, PPAR signaling pathway, ECM-receptor interaction, carbon metabolism and AMPK signaling pathway.

In the low-vs. high-IMF comparison, GO analysis of DEGs from low- and high-IMF pigs showed that 164 BPs, 12 CCs, and 20 MFs were significantly enriched (Supplementary Table S10). KEGG enrichment analysis showed 14 significantly enriched pathways (Supplementary Table S11). The top 10 GO and KEGG terms are shown in Fig. 3B and D. GO functional enrichment analysis showed that DEGs were mainly involved in the negative regulation of lipid metabolic process, regulation of lipid metabolic process, Rac protein signal transduction, regulation of bone remodeling, lipid catabolic process, regulation of tissue remodeling and negative regulation of protein modification process. KEGG pathway analysis revealed that DEGs were significantly enriched in metabolic pathways, fatty acid elongation/metabolism, biosynthesis of unsaturated fatty acids, valine, leucine and isoleucine degradation and carbon metabolism.

3.3. PPI network construction and hub genes identification

From the BT group, 56 integrated DEGs were analyzed via the STRING online database to construct a PPI network consisting of 17 nodes and 16 edges, as shown in Fig. 3E. And the top 10 genes with the highest MCC scores were identified as hub genes, which were shown in Fig. 3G. The GO analysis revealed that 10 hub genes were primarily enriched in the secretory granule, oxidation-reduction process (Fig. 3I–Supplementary Table S12). KEGG terms were enriched in metabolic pathways, fatty acid metabolism, PPAR signaling pathway, carbon metabolism and AMPK signaling pathway were intimately related to the fat metabolism process (Fig. 3K–Supplementary Table S12). Subsequently, the intersection of the 10 hub genes and the merge dataset in the BT group revealed that only seven genes (*SCD*, *ACLY*, *ME1*, *FASN*, *HK2*, *ARVCF* and *TXNRD2*) were obtained as hub genes for the following analysis. Finally, correlation analysis showed a significant positive correlation between the expression levels of *ACLY*, *ME1*, *FASN* and *HK2* (Fig. 3M).

In the low-vs. high-IMF comparison, an interaction network of 52 integrated DEGs, consisting of 17 nodes and 16 edges, was constructed as shown in Fig. 3F. And the top 10 genes with the highest MCC scores were identified as hub genes, which were shown in Fig. 3H. The GO analysis revealed that 10 hub genes were primarily enriched in the mitochondrion organization, lipid metabolic

process (Fig. 3J–Supplementary Table S13). Also, KEGG analysis showed that hub genes were enriched in valine, leucine and isoleucine degradation, peroxisome, carbon metabolism, apelin signaling pathway and metabolic pathways (Fig. 3L–Supplementary Table S13). Subsequently, the intersection of the 10 hub genes and the merge dataset in the IMF group was found to be obtained for nine genes (*CEBPA*, *ELOVL6*, *PLIN1*, *CIDEC*, *CAST*, *ACTA2*, *CREM*, *HMGCL* and *PCCB*) as hub genes for the following analysis. Finally, the correlation analysis showed a significant positive correlation between the expression levels of *CEBPA*, *ELOVL6* and *PLIN1* genes. In addition, the expression level of *ACTA2* showed a negative correlation with that of *CAST* and a positive correlation with that of *PCCB* (Fig. 3N).

3.4. Screening and verification of potential biomarker

From the merged dataset in the BT group, machine learning approach was utilized to further investigate potential biomarkers associated with SA deposition in the hub genes. The LASSO regression algorithm yielded four potential candidate biomarkers (Fig. 4A). SVM–REF analysis revealed that the model incorporating seven genes had the best accuracy (Fig. 4B). In addition, the Random Forest algorithm ranked the genes based on the calculation of the importance of each gene (Fig. 4C). Finally, the intersection of the four potential candidate genes from LASSO, seven potential candidate genes from SVM-REF and the top five most important genes from the Random Forest was visualized via the Venn diagram, yielding *ACLY*, *FASN*, *ME1* and *ARVCF* in the BT group as SA deposition-related potential biomarkers (Fig. 4D). We then used a validation set, GSE61271, as an independent dataset to validate the SA deposition-related potential biomarkers obtained above for reliability. As shown in Fig. 4I-L, only *FASN* showed significantly higher expression in the high-BT pigs. Meanwhile, the validation dataset GSE61271 was also used to validate the effectiveness of *ACLY*, *FASN*, *ME1* and *ARVCF* by ROC analysis, the AUCs of *ACLY*, *FASN*, *ME1* and *ARVCF* were 0.61, 0.75, 0.68 and 0.72, respectively (Fig. 4I-L). Based on validation results, *FASN* as a potential biomarker showed excellent specificity and sensitivity in SA tissue between low- and high-BT pigs. GSEA functional analysis of four potential biomarkers detected multiple significant pathways (Fig. 5A–D)

From the merged datasets in the IMF group, the LASSO regression algorithm yielded four potential candidate biomarkers (Fig. 4E). The SVM-REF analysis revealed that the model incorporating four genes had the best accuracy (Fig. 4F). In addition, the Random Forest

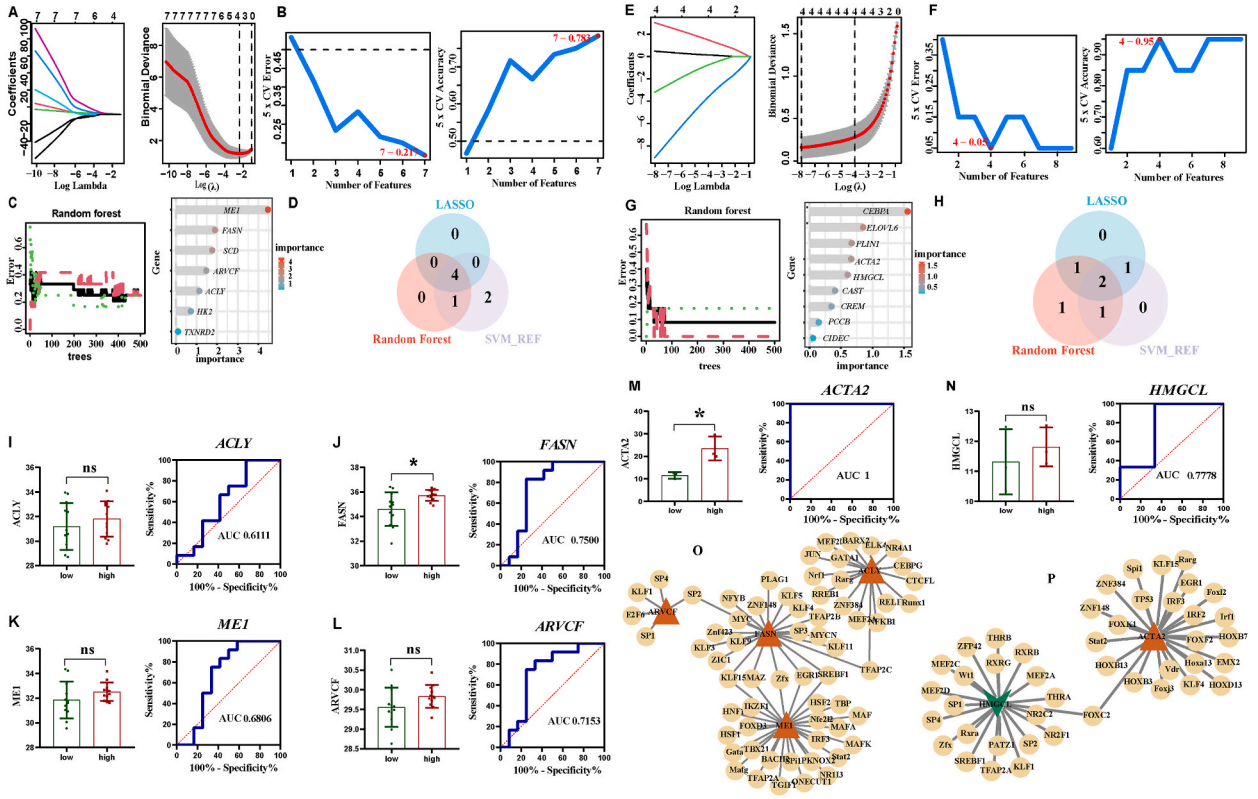

Fig. 4. Potential tissue-specific biomarkers detection, validation and analysis. (A–C) The machine learning algorithms, in order, was the LASSO, SVM-REF, and Random Forest to screen potential biomarkers in BT group. (D) Venn diagram showed the overlap of potential biomarkers identified by the three algorithms in BT group. Barplot showed the expression of biomarkers between low- and high-BT group in validation set, the ROC curve of the efficacy verification of biomarkers (I) *ACLY*, (J) *FASN*, (K) *ME1*, (L) *ARVCF*. (B–G) The machine learning algorithms in IMF group. (H) Venn diagram in IMF group. Barplot and ROC curve of potential biomarkers (M) *ACTA2*, (N) *HMGCL* in IMF group. (O–P) The network of TFs and potential biomarkers in BT group and IMF group. *$P < 0.05$, **$P < 0.01$, ns, no significant difference.

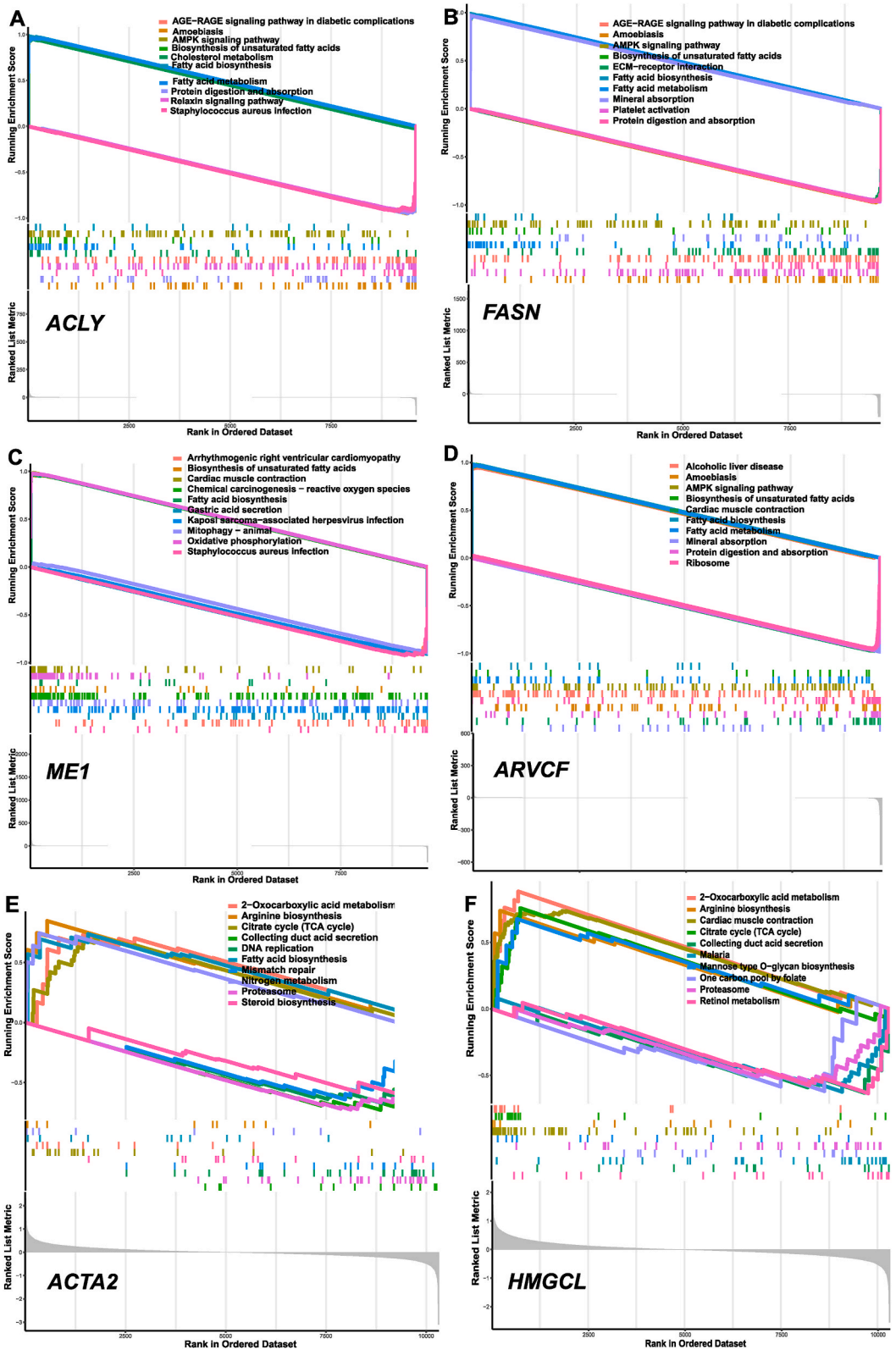

Fig. 5. The GSEA of potential biomarkers. (A) *ACLY*. (B) *FASN*. (C) *ME1*. (D) *ARVCF*. (E) *ACTA2*. (F) *HMGCL*.

algorithm ranked the genes (Fig. 4G). Finally, *ACTA2* and *HMGCL* were obtained as potential biomarkers of IMF deposition from gene intersections obtained by three machine learning algorithms (Fig. 4H). The GSE180840 dataset was then used to validate the accuracy of the biomarkers. As shown in Fig. 4M – N, only *ACTA2* was significantly upregulated in high-IMF pigs. The AUCs of *ACTA2* and *HMGCL* were 1 and 0.78, respectively (Fig. 4M – N). According to the validation results, *ACTA2*, which had a significant difference in expression levels between high- and low-IMF pigs and a high AUC was considered to be the most specific and sensitive potential IMF deposition-specific biomarker. The GSEA analysis results for *ACTA2* and *HMGCL* were shown in Fig. 5E and F.

3.5. Analysis of gene regulatory network for potential tissue-specific biomarkers

In the SA deposition-related latent biomarkers, a total of 63 transcription factors (TFs) were predicted based on the four latent biomarkers, including 17 TFs predicted by *ACLY*, 21 TFs predicted by *FASN*, 27 TFs predicted by *ME1,* and 5 TFs predicted by *ARVCF* (Fig. 4O). The results showed that *FASN* has the most common TFs with the other biomarkers, especially with the ME1.

For potential biomarkers related to IMF deposition, a total of 44 TFs were predicted based on two potential biomarkers, including 24 TFs predicted by *ACTA2* and 21 TFs predicted by *HMGCL* (Fig. 4P). *ACTA2* and *HMGCL* shared a common TF, *FOXC2*.

3.6. Analysis of ceRNA network for potential tissue-specific biomarkers

For the SA deposition-related latent biomarkers (*ACLY, FASN, ME1 and ARVCF*), a total of 16 lncRNA of 20 miRNA of four biomarkers were predicted, which were paired into 170 lncRNA-miRNA interactions, and 20 miRNA-mRNA interactions (Fig. 6A). For the IMF deposition-related biomarkers (*ACTA2* and *HMGCL*), a total of nine lncRNA of seven miRNA of two biomarkers were predicted, which were paired into 24 lncRNA-miRNA interactions, and seven miRNA-mRNA interactions (Fig. 6B). Based on the forecasted results of miRNAs and lncRNAs of tissue-specific biomarkers, we found that lncRNA NEAT1 and XIST could sponge different miRNAs to regulate tissue-specific genes association with fat deposition of SA and IMF, respectively.

3.7. Phenotypes for the experimental pigs of qRT-PCR validation

Information on the test animals, including characteristics related to fat deposition, is given in Table 2. In the BT group, the carcass BT level of Saba pigs at high-BT pigs was significantly higher than that in the low-BT pigs ($P < 0.01$), the carcass BT level ($P < 0.01$) and IMF content ($P < 0.05$) of Saba pigs was significantly higher than that in the Large White pigs. In the IMF group, the IMF content of Saba pigs at high-IMF pigs was significantly higher than that in the low-IMF pigs ($P < 0.01$), the carcass BT level and IMF content of Saba pigs was significantly higher than that in the Large White pigs ($P < 0.01$).

3.8. Validation of the biomarkers by qRT-PCR

The expression trends for the potential tissue-specific biomarkers were broadly consistent with the RNA sequencing results in the datasets, in particular *FASN* in high-BT pigs and *ACTA2* in high-IMF pigs were significantly upregulated in RNA-seq, validation and

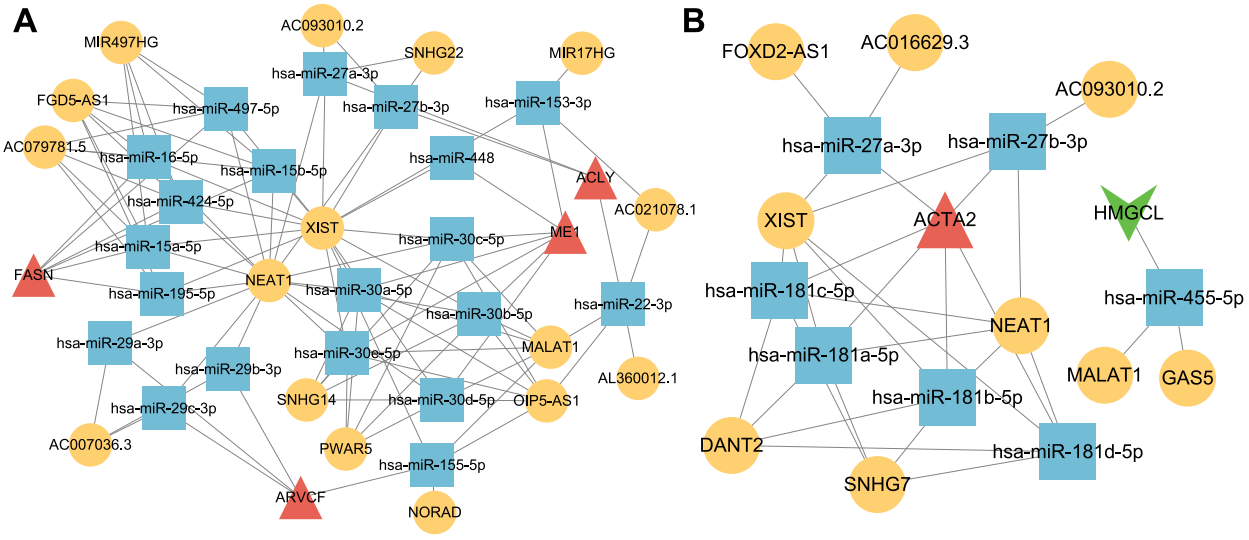

Fig. 6. The integrated ceRNA network. (A) ceRNA network of lncRNA, miRNA, and SA deposition-related biomarkers. (B) ceRNA network of lncRNA, miRNA, and IMF deposition-related biomarkers. Red triangle: up-regulated biomarkers. Green arrow: down-regulated biomarkers. Yellow circle: lncRNA. Blue square: miRNA. (For interpretation of the references to color in this figure legend, the reader is referred to the Web version of this article.)

Table 2
The traits were compared between the Saba pigs with low- and high-BT, Large White and Saba pigs, Saba pigs with low- and high-IMF, which the capital and lowercase letters indicate $P < 0.01$ and $P < 0.05$, respectively.

Validation	Group	n	Live weight (kg)	Carcass BT (mm)	IMF (%)
SA deposition-related biomarkers	Saba pigs with low-BT	3	102.50 ± 6.75	38.25 ± 1.85A	4.64 ± 1.57
	Saba pigs with high-BT	3	102.33 ± 4.03	56.94 ± 1.98B	5.54 ± 1.37
	Large White pigs	3	100.08 ± 1.17	22.95 ± 5.83A	2.67 ± 0.94a
	Saba pigs	3	102.33 ± 4.03	56.94 ± 1.98B	5.54 ± 1.37b
IMF deposition-related biomarkers	Saba pigs with low-IMF	3	100.67 ± 1.25	53.62 ± 4.27	2.43 ± 0.27A
	Saba pigs with high-IMF	3	107.67 ± 4.03	46.98 ± 2.27	9.01 ± 0.74B
	Large White pigs	3	100.50 ± 1.47	25.37 ± 5.84A	2.80 ± 0.70A
	Saba pigs	3	107.67 ± 4.03	46.98 ± 2.27B	9.01 ± 0.74B

qPCR data, except for *HMGCL* where qRT-PCR validation was not consistent with the sequencing results (Fig. 7A–D). The expression level of these tissue-specific biomarkers was detected in both SA and IMF tissues to exclude the universality (Fig. 7A–D). The results revealed that biomarkers associated with SA deposition (*ACLY*, *FASN*, and *ARVCF*) and IMF deposition (*ACTA2*) appeared to have better sensitivity and specificity.

4. Discussion

The amount of SA and IMF deposition are critical factors affecting pork production and eating quality, and are also strongly associated with obesity and metabolism obstacle disease [29,30]. While increasing number of functional genes which play important role in fat deposition have been screened with the development of high-throughput sequencing technology, finding tissue-specific biomarkers related with fat deposition is a critical step in understanding the mechanisms of fat deposition in different tissue to regulate the content of fat and explore the potential therapeutic targets for metabolic diseases associated with obesity. Our results are generally consistent with and extend those of prior fat deposition studies. In our study, we systematically compared and analyzed the molecular regulatory mechanisms affecting SA and IMF deposition, and identified tissue-specific biomarkers involved in fat deposition using the RRA method combining respectively with multiple datasets related to SA and IMF deposition. At the same time, the

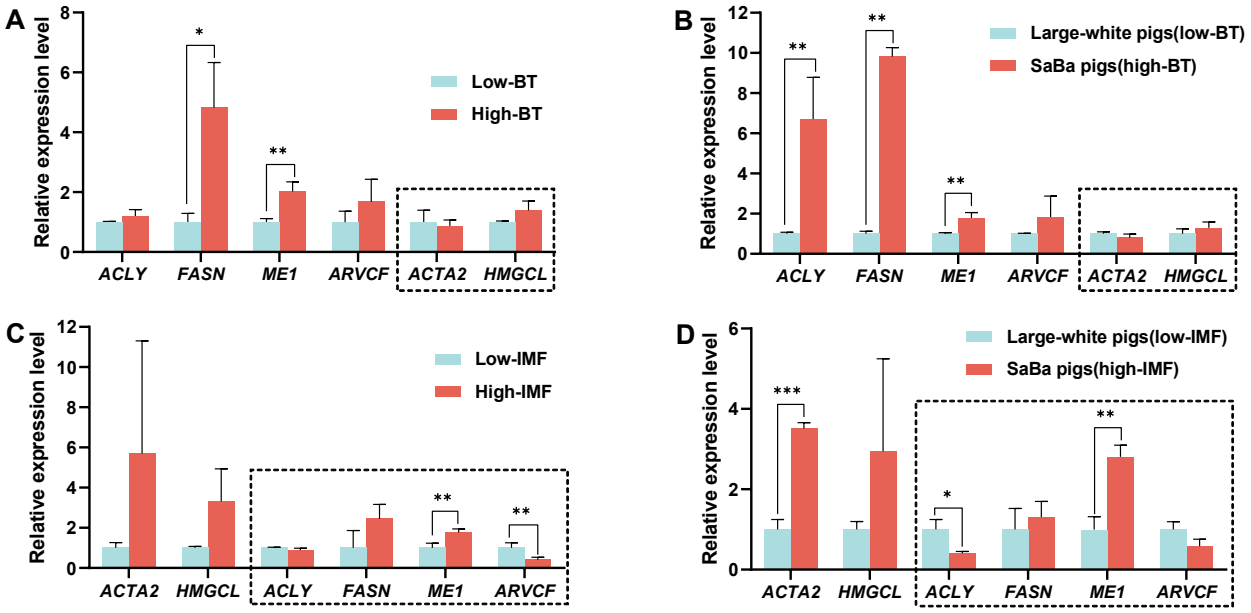

Fig. 7. Validation of potential biomarkers through qRT-PCR. (A) The same breed with low- and high-BT pigs as the test animals. mRNA expression of SA deposition-related biomarkers *ACLY*, *FASN*, *ME1*, and *ARVCF* showed the same trend with the results of bioinformatics analysis in datasets. *FASN* and *ME1* showed significant difference. IMF deposition-related biomarkers *ACTA2* and *HMGCL* showed the opposite trend. (B) The Large white (low-BT) and Saba (high-BT) pigs as the test animals. mRNA expression of *ACLY*, *FASN*, *ME1*, and *ARVCF* showed the same trend. *ACLY*, *FASN*, and *ME1* showed significant difference. While *ACTA2* and *HMGCL* showed the opposite trend. (C) The same breed with low- and high-IMF pigs as the test animals. mRNA expression of IMF deposition-related biomarkers *ACTA2* showed the same trend, but *HMGCL* was opposite. SA deposition-related biomarkers *ACLY* and *ARVCF* showed the opposite trend, but *FASN* and *ME1* showed the same trend. (D) The Large white (low-IMF) and Saba (high-IMF) pigs as the test animals. *ACTA2* showed the same trend and significantly higher than large white pigs compared with Saba pigs, but HMGCL was opposite. *ACLY* and *ARVCF* showed the opposite trend, but *FASN* and *ME1* showed the same trend. $^{*}P < 0.05$, $^{**}P < 0.01$, $^{***}P < 0.001$.

prediction of TFs, lncRNAs and miRNAs targeting the biomarkers were performed for further investigating the potential regulatory mechanism.

4.1. Potential biomarkers involved in subcutaneous fat deposition

Fifty-six DEGs were filtered out, with 27 down- and 29 up-regulated genes in the BT group. Functional analysis of these DEGs indicated that these targets were primarily associated with the synthesis and metabolism of fats and fatty acids, the energy balance of the organism, such as the carboxylic acid metabolic/biosynthetic process [31], PPAR signaling pathway [32], ECM-receptor interaction [33] and AMPK signaling pathway [34]. These pathways aberrant expression genes mainly contained *FASN*, *ME1* and *ACLY* among the DEGs. We also constructed PPI networks to obtain 10 hub genes. Among these hub genes, *ACLY*, *FASN*, *ME1* and *ARVCF* were then screened as potential SA deposition-specific biomarkers using bioinformatics and three machine learning approaches. In particular, *FASN* was identified as the most sensitive biomarker and might play a vital role in the fat deposition process in SA.

ACLY (ATP citrate lyase) is a crucial enzyme in fatty acid synthesis and cholesterol biosynthesis, which play a vital role in modulating carcass and muscle fat content [35]. *ACLY* can influence the synthesis and deposition of fatty acids in SA by regulating the level of acetyl coenzyme A, an essential precursor to the synthesis of fatty acids and triacylglycerols [36]. In addition, *ACLY* has been shown to activate SREBP-1c, a key regulator of lipid metabolism, by promoting its nuclear localization and enhancing its transcriptional activity, thereby increasing fatty acid synthesis in subcutaneous adipocytes and promoting fat deposition [37,38]. Besides, the genes, *ACLY*, *FASN* and *ME1*, all of which play crucial roles in de novo fatty acid biosynthesis, elongation and desaturation, are found to be significantly up-regulated in the SA of fat breeds, indicating that they are critically involved in SA deposition [39].

ME1 (malic enzyme 1) is a cytosolic $NADP^+$-dependent enzyme that plays a critical role in NADPH production, fatty acid biosynthesis and lipogenesis in cells and tissues [40]. *ME1* also plays a considerable role in glucose metabolism to the initial steps of lipogenesis [41]. In addition, *ME1* activity and expression levels are regulated by several factors, including hormones such as insulin and glucagon, as well as nutritional factors. For example, *ME1* expression levels in adipocytes increases with high-fat feeding [42]. Some previous studies have shown that *ME1* expression levels and activity were related to the BT in pigs. For instance, Ramı'rez et al. found that *ME1* activity in Iberian × Duroc hybrids was positively correlated with BT and IMF content [43]. Xing discovered that *ME1* was significantly associated with BT at 171 days in Landrace pigs, and expression levels were more abundant in pigs with high BT [44]. *ME1* expression levels were also found to significantly impact leanness in turkeys and regulate fat deposition in yak [45,46]. Our results are consistent with previous studies and again confirm that *ME1* plays a critical role in SA deposition. The Armadillo Repeat gene deleted in Velo-Cardio-Facial syndrome (*ARVCF*) is a member of the vertebrate p120 catenin subfamily that responds to components of the canonical WNT pathway, which plays an important role in adipocyte differentiation and fatty acid synthesis [47]. Currently, primary research on *ARVCF* has focused on gene function, such as influencing the splicing of specific pre-mRNAs, and human diseases, such as schizophrenia and tumors [48,49]. The role of *ARVCF* in fat deposition is largely unstudied. GSEA pathway-based analyses implicated *ARVCF* in fatty acid metabolism, such as the AMPK signaling pathway, biosynthesis of unsaturated fatty acids. Thus, we speculate that *ARVCF* may be implicated in the subcutaneous fat deposition process in pigs.

FASN (fatty acid synthase), a critical adipogenic gene, plays a key role in de novo fatty acid synthesis as the main long-chain fatty acid synthesizer [50]. In addition, *FASN* mediates de novo lipid synthesis via catalyzing the production of palmitate from acetyl-coenzyme A (CoA), malonyl-CoA and *NADPH* [51], and the palmitate is the precursor of major nutritional, energetic and signaling lipids [52]. Besides, *FASN* can be regulated by PPAR-γ and SREBP-1C, which are the key TFs for adipocyte differentiation and lipid accumulation, thus regulating fatty acid synthesis [53]. *FASN* also participates in regulating adipocyte differentiation and the formation of mature adipocytes, and promotes differentiation of pre-adipocytes into mature adipocytes, which contributes to the formation of adipose tissue [54]. Previous studies have shown that elevated levels of *FASN* significantly increased triglyceride deposition in the body, leading to obesity [55]. *FASN* is highly expressed in porcine adipose tissue, with positive correlations between *FASN* expression and carcass adipose content in pigs [56]. It was also found that the expression of *FASN* was up-regulated at higher BT and had a positive regulatory effect on BT in pigs, consistent with its fat-accumulating function found in previous studies [57–59]. But, remarkably, the previous study alsofound that *FASN* expression levels were negatively correlated with IMF contents in the LDM of Kazak sheep [60]. In the current study, we found that *FASN* might specifically regulate fat deposition in pigs with SA, with a positive relationship between *FASN* expression levels and BT. Moreover, qRT-PCR validated gene expression levels in both low and high BT pigs and lean and obese pigs of the same breed showed high agreement with transcriptome sequencing, all suggesting that *FASN* was significantly higher in high BT pigs. Although we also found that the expression of *FASN* was relatively low in high-IMF pigs compared to low-IMF pigs in LDM, this was not significant, indicating that *FASN* might have different activity in different species to stimulate adipose accumulation. Therefore, we speculated that *FASN* has a great possibility to be a critical gene in SA deposition process, but its specific mechanism and function needs more experiment verification.

The bio-functional analysis of the GSEA of *ACLY*, *FASN*, *ME1* and *ARVCF* detected the synthesis and metabolism of fats and fatty acids, energetic balance of the organism-related pathways such as AMPK signaling pathway [61], biosynthesis of unsaturated fatty acids [62], suggesting that these biomarkers may effect these pathways to mediate the regulation of energy metabolism in porcine adipocytes of SA to regulate fat deposition. In addition, the expression level of *FASN* was positively correlated with those of *ACLY* and *ME1*. Moreover, we also explored the regulatory mechanisms of these potential biomarkers, and *FASN* has commonalities with other biomarkers in TFs, particularly *ME1*. *FASN* and *ME1* were found to have higher levels of gene expression in mice fed a high-fat diet [63] and these genes were transcriptionally regulated by ChREBP belong to lipid synthesis genes [64]. Following discovering possible tissue-specific biomarkers for fat deposition, we also predicted the miRNAs and lncRNAs linked to biomarkers and constructed ceRNA networks to connect them. From the mRNA–miRNA interaction, we found that *FASN* interact with different fat metabolism-related

miRNAs such as miR-15a-5p [65], miR-16-5p [66], miR-424-5p [67] and miR-497-5p [68]. Also, it is notable that lncRNA XIST and NEAT1 were predicted to regulate *FASN* through miRNA mentioned above, respectively. Since many investigations pointed out that the XIST and NEAT1 are the key players in regulation of lipid metabolism [69,70], we postulated that the role of ceRNA interaction network of XIST, NEAT1/miR-15a-5p, miR-16-5p, miR-424-5p, miR-497-5p/*FASN* are vital in the SA metabolism, which may give suggestions for regulation of fat deposition.

4.2. Potential biomarkers involved in IMF deposition

Fifty-two DEGs were filtered out and 18 down- and 34 up-regulated genes were presented in the IMF group. Functional analysis of these DEGs showed that these targets were primarily associated with lipid metabolism, energy metabolites and amino acid biosynthesis and degradation, such as lipid metabolic process [71], valine, leucine and isoleucine degradation [72], peroxisome [73], apelin signaling pathway [74]. Subsequently, *ACTA2* and *HMGCL* were screened as potential biomarkers specific to IMF deposition through bioinformatics and three machine learning approaches, with *ACTA2* in particular identified as the most potentially sensitive biomarker.

ACTA2 (alpha-smooth muscle actin) is a gene encoding alpha-smooth muscle actin (αSMA) and identified as a marker of myofibroblast formation [75]. Additionally, it has been suggested that *ACTA2* might act an important role in the regulation of intramuscular adipocyte differentiation and lipid metabolism. Such as *ACTA2* contributes to the formation of adipocytes under certain conditions [76,77]. A previous study showed that *ACTA2*-positive myofibroblasts could regenerate de novo adipocytes [78]. In addition, *ACTA2* has been shown to be involved in the differentiation of adipocytes and smooth muscle cells through the regulation of myocyte-associated transcription factor-A (MRTF-A) [79]. Besides, it was reported that *ACTA2* was highly expressed in LDM of Xinjiang brown cattle with higher fat percentage and larger area of LDM, and better beef tenderness compared with Kazakh cattle, indicated that *ACTA2* exerted a crucial regulatory impact on the composition and characteristics of adipose and meat quality [80]. In our study, *ACTA2* showed a significantly high level only in the LDM of pigs with high IMF, differences in the expression level of *ACTA2* may be an important reason for the degrees of differentiation of adipocytes of adipocytes in adipose tissues at different sites. Thus, we speculated that *ACTA2* could potentially be used as a biomarker to regulate the IMF metabolism, but more investigations are needed to identify specific mechanisms.

HMGCL (3-hydroxy-3-methylglutaryl-CoA lyase), which encodes a protein belonging to the HMG-CoA lyase family, is widely implicated in butanoate metabolism, synthesis and degradation of ketone body, and valine, leucine, and isoleucine degradation [81]. Meanwhile, *HMGCL* has also been reported to be connected with lipid metabolism [82]. Several studies have reported that *HMGCL* might play a critical role in regulating SA deposition in pigs by being involved in the synthesis and degradation of ketone bodies and propanoate metabolism, but limited work has been done to validate this function in fat deposition [11]. In our study, the expression of the *HMGCL* gene was significantly downregulated compared to that in low-IMF pigs from the dataset analysis. However, the expression level of the *HMGCL* was relatively high in the high-IMF pigs in the validation dataset and in the qPCR results compared to the low-IMF pigs. This variation is most likely related to differences in pig breeds, but further researches are required to identify the function of *HMGCL* in IMF deposition.

Bio-functional analysis of the GSEA of *ACTA2* and *HMGCL* detected lipid metabolism, amino acid biosynthesis and degradation-related pathways such as fatty acid metabolism [83] and biosynthesis of amino acids, alanine, aspartate and glutamate metabolism [84], which were largely concordant with the results of our previous DEG functional analysis results. We also identified signaling pathways involved in the regulation of protein synthesis, such as protein processing in the endoplasmic reticulum [85].Furthermore, we inferred a regulatory network by connecting predictive TFs with the biomarkers *ACTA2* and *HMGCL*. The results showed that *ACTA2* shared a common TF *FOXC2* with *HMGCL*. *FOXC2* is a forkhead TF that plays an essential role in lipid metabolism, muscle tube formation and vascular remodeling in muscle tissue [86]. Previous studies have shown that *FOXC2* had the ability to block adipogenesis by increasing the activity of the β-adrenergic-cAMP-protein kinase A (PKA) signaling pathway and by inhibiting *PPARG* to promote the expression of mature adipocyte genes [87,88]. Further studies are also needed to define the mechanism of association with *FOXC2*. From the mRNA–miRNA interaction, we found that *ACTA2* interact with different fat metabolism and adipocyte differentiation-related miRNAs such as miR-27a/b-3p [89–91], miR-181a/c-5p [92]. It is also found that circRNA XIST and NEAT1 were predicted to regulate *ACTA2* through miRNA mentioned above. Therefore, we postulated that the ceRNA interaction network of XIST, NEAT1/miR-27a/b-3p, 181a/c-5p/*ACTA2* may contribute to the regulation to IMF metabolism. Certainly, further experimental analysis is needed for all potential interactions among biomarkers, miRNAs, and lncRNAs.

Although potential tissue-specific biomarkers related to fat deposition have beenscreened, and some genes have been validated in previous studies, some limitations of the current study must be noted. Firstly, the potential biomarkers were obtained through bioinformatics method. Moreover, the regulation mechanism targeting fat deposition has not been experimentally validated. Secondly, the specific functions and expression pattern of the biomarkers need to be verified in cells or animals using overexpression or knockdown methods. Therefore, although our results were validated in multi-datasets and qPCR, further trials are needed to affirm the value of tissue-specific biomarkers.

5. Conclusions

We identified four SA genes related to AMPK signaling pathway, PPAR signaling pathway and biosynthesis of unsaturated fatty acids, and 2 IMF genes related to fatty acid metabolism and biosynthesis of amino acids, alanine, aspartate and glutamate metabolism, displayed a tissue-specific association with BT and IMF content, respectively. Moreover, the predicted RNA pathways of XIST, NEAT1/

miR-15a-5p, miR-16-5p, miR-424-5p, miR-497-5p/*FASN* and XIST, NEAT1/miR-27a/b-3p, 181a/c-5p/*ACTA2* may contribute to the regulation to SA and IMF metabolism, respectively. Collectively, this study provides reliable molecular biomarkers for the analysis of fat deposition in SA and IMF. It also lays the foundation for meat quality improvement in pig breeding.

Ethics declaration

This study was reviewed and approved by the Animal Ethics Committee of Yunnan Agricultural University, with the approval number: 202310003.

Funding support

This work was supported by Yunnan Swine Industry Technology System Program (2020KJTX0016), Yunnan Province Important National Science & Technology Specific Projects (202104BI090022, 202102AE090039).

Data availability statement

The transcriptome datasets analyzed during the current study are available in the public NCBI GEO database (https://www.ncbi.nlm.nih.gov/geo/). Accession number: GSE122349, GSE145956, GSE61271, GSE165613, GSE207279 and GSE180840.

CRediT authorship contribution statement

Yongli Yang: Writing – original draft, Visualization, Methodology, Data curation. **Mingli Li:** Writing – original draft, Methodology, Data curation. **Yixuan Zhu:** Visualization, Validation. **Xiaoyi Wang:** Visualization, Validation, Methodology. **Qiang Chen:** Validation, Data curation. **Shaoxiong Lu:** Writing – review & editing, Funding acquisition.

Declaration of competing interest

The authors declare that they have no known competing financial interests or personal relationships that could have appeared to influence the work reported in this paper.

Acknowledgements

We warmly thank the assistance of Chuxiong Prefecture Pig Breeding Farm and Yunnan Fuyuefa Livestock and Poultry Feeding Company Limited staff in experimental pigs selecting, particularly Drs Wenhui Ren and Yanlin Zhang.

Appendix A. Supplementary data

Supplementary data to this article can be found online at https://doi.org/10.1016/j.heliyon.2024.e31311.

Abbreviations

BT	Backfat thickness
IMF	intramuscular fat
SA	subcutaneous adipose
RRA	robust rank aggregation
PPI	protein-protein interaction
ROC	receiver operating characteristic
GEO	Gene Expression Omnibus
DEGs	Differentially expressed genes
GO	gene ontology
BPs	biological processes
CCs	cellular components
MFs	molecular functions
KEGG	Kyoto Encyclopedia of Genes and Genomes
GSEA	Gene set enrichment analysis
MCC	Maximal Clique Centrality
LASSO	least absolute shrinkage and selection operator
SVM-REF	support vector machine-recursive feature elimination
AUC	area under curves

References

[1] K. Suzuki, M. Irie, H. Kadowaki, T. Shibata, M. Kumagai, A. Nishida, Genetic parameter estimates of meat quality traits in Duroc pigs selected for average daily gain, longissimus muscle area, backfat thickness, and intramuscular fat content, J. Anim. Sci. 83 (9) (2005) 2058–2065, https://doi.org/10.2527/2005.8392058x.

[2] P. Zhang, Y. Fu, R. Zhang, P. Shang, H. Zhang, B. Zhang, Association of KCTD15 gene with fat deposition in pigs, J. Anim. Physiol. Anim. Nutr. 106 (3) (2022) 537–544, https://doi.org/10.1111/jpn.13587.

[3] M.P. Robich, R.M. Osipov, R. Nezafat, J. Feng, R.T. Clements, C. Bianchi, M. Boodhwani, M.A. Coady, R.J. Laham, F.W. Sellke, Resveratrol improves myocardial perfusion in a swine model of hypercholesterolemia and chronic myocardial ischemia, Circulation 122 (11) (2010) S142–S149, https://doi.org/10.1161/circulationaha.109.920132.

[4] M.E. Spurlock, N.K. Gabler, The development of porcine models of obesity and the metabolic syndrome, J. Nutr. 138 (2) (2008) 397–402, https://doi.org/10.1093/jn/138.2.397.

[5] J.S. Samra, Regulation of lipid metabolism in adipose tissue, Proc. Nutr. Soc. 59 (3) (2000) 441–446, https://doi.org/10.1017/s0029665100000604.

[6] G. Zhou, S. Wang, Z. Wang, X. Zhu, G. Shu, W. Liao, K. Yu, P. Gao, Q. Xi, X. Wang, Y. Zhang, L. Yuan, Q. Jiang, Global comparison of gene expression profiles between intramuscular and subcutaneous adipocytes of neonatal landrace pig using microarray, Meat Sci. 86 (2) (2010) 440–450, https://doi.org/10.1016/j.meatsci.2010.05.031.

[7] H. Sauerwein, E. Bendixen, L. Restelli, F. Ceciliani, The Adipose tissue in farm animals: a proteomic approach, Curr. Protein Pept, Science 15 (2) (2014) 146–155, https://doi.org/10.2174/1389203715666140221123105.

[8] J.F. Hocquette, F. Gondret, E. Baeza, F. Medale, C. Jurie, D.W. Pethick, Intramuscular fat content in meat-producing animals: development, genetic and nutritional control, and identification of putative markers, Animal 4 (2) (2010) 303–319, https://doi.org/10.1017/s1751731109991091.

[9] M. Kouba, M. Bonneau, Compared development of intermuscular and subcutaneous fat in carcass and primal cuts of growing pigs from 30 to 140 kg body weight, Meat Sci. 81 (1) (2009) 270–274, https://doi.org/10.1016/j.meatsci.2008.08.001.

[10] P. Zhang, B. Zhang, P. Shang, Y. Fu, R. Nie, Y. Chamba, H. Zhang, Comparative transcriptomic profiles of differentiated adipocytes provide insights into adipogenesis mechanisms of subcutaneous and intramuscular fat tissues in pigs, Cells 11 (3) (2022) 499, https://doi.org/10.3390/cells11030499.

[11] P. Zhang, Q. Li, Y. Wu, Y. Zhang, B. Zhang, H. Zhang, Identification of candidate genes that specifically regulate subcutaneous and intramuscular fat deposition using transcriptomic and proteomic profiles in Dingyuan pigs, Sci. Rep. 12 (1) (2022) 2844, https://doi.org/10.1038/s41598-022-06868-3.

[12] Y. Zhang, Y. Sun, Z. Wu, X. Xiong, J. Zhang, J. Ma, S. Xiao, L. Huang, B. Yang, Subcutaneous and intramuscular fat transcriptomes show large differences in network organization and associations with adipose traits in pigs, Sci. China Life Sci. 64 (10) (2021) 1732–1746, https://doi.org/10.1007/s11427-020-1824-7.

[13] C. Yao, D. Pang, C. Lu, A. Xu, P. Huang, H. Ouyang, H. Yu, Data mining and validation of AMPK pathway as a novel candidate role affecting intramuscular fat content in pigs, Animals 9 (4) (2019) 137, https://doi.org/10.3390/ani9040137.

[14] H.T. Liu, K. Xing, Y.F. Jiang, Y.B. Liu, C.D. Wang, X.D. Ding, Using machine learning to identify biomarkers affecting fat deposition in pigs by integrating multisource transcriptome information, J. Agric. Food Chem. 70 (33) (2022) 10359–10370, https://doi.org/10.1021/acs.jafc.2c03339.

[15] X. Wang, S.L. Shi, G.J. Wang, W.X. Luo, X. Wei, A. Qiu, F. Luo, X.D. Ding, Using machine learning to improve the accuracy of genomic prediction of reproduction traits in pigs, J. Anim. Sci. Biotechnol. 13 (1) (2022) 60, https://doi.org/10.1186/s40104-022-00708-0.

[16] M.E. Ritchie, B. Phipson, D. Wu, Y.F. Hu, C.W. Law, W. Shi, G.K. Smyth, Limma powers differential expression analyses for RNA-sequencing and microarray studies, Nucleic Acids Res. 43 (7) (2015) e47, https://doi.org/10.1093/nar/gkv007.

[17] R. Kolde, S. Laur, P. Adler, J. Vilo, Robust rank aggregation for gene list integration and meta-analysis, Bioinformatics 28 (4) (2012) 573–580, https://doi.org/10.1093/bioinformatics/btr709.

[18] J.T. Leek, W.E. Johnson, H.S. Parker, A.E. Jaffe, J.D. Storey, The sva package for removing batch effects and other unwanted variation in high-throughput experiments, Bioinformatics 28 (6) (2012) 882–883, https://doi.org/10.1093/bioinformatics/bts034.

[19] C.H. Chin, S.H. Chen, H.H. Wu, C.W. Ho, M.T. Ko, C.Y. Lin, cytoHubba: identifying hub objects and sub-networks from complex interactome, BMC Syst. Biol. 8 (4) (2014) 1–7, https://doi.org/10.1186/1752-0509-8-S4-S11.

[20] R. Tibshirani, Regression shrinkage and selection via the lasso, J. Roy. Stat. Soc. 58 (1) (1996) 267–288, https://doi.org/10.1111/j.2517-6161.1996.tb02080.x.

[21] J.A.K. Suykens, J. Vandewalle, Least squares support vector machine classifiers, Neural Process. Lett. 9 (3) (1999) 293–300, https://doi.org/10.1023/a:1018628609742.

[22] Breiman, Random forests, Mech Learn 45 (1) (2001) 5–32, 2001.

[23] J. Friedman, T. Hastie, R. Tibshirani, Regularization Paths for Generalized linear models via coordinate descent, J. Stat. Software 33 (1) (2010) 1–22, https://doi.org/10.18637/jss.v033.i01.

[24] M.L. Huang, Y.H. Hung, W.M. Lee, R.K. Li, B.R. Jiang, SVM-RFE based feature selection and taguchi parameters optimization for multiclass SVM classifier, Sci. World (2014) 1–10, https://doi.org/10.1155/2014/795624.

[25] S.J. Rigatti, Random forest, J. Insur. Med. 47 (1) (2017) 31–39, https://doi.org/10.17849/insm-47-01-31-39.1.

[26] L. Salmena, L. Poliseno, Y. Tay, L. Kats, P.P. Pandolfi, A ceRNA hypothesis: the rosetta stone of a hidden RNA language? Cell 146 (3) (2011) 353–358, https://doi.org/10.1016/j.cell.2011.07.014.

[27] D. Betel, A. Koppal, P. Agius, C. Sander, C. Leslie, Comprehensive modeling of microRNA targets predicts functional non-conserved and non-canonical sites, Genome Biol. 11 (8) (2010) 1–16, https://doi.org/10.1186/gb-2010-11-8-r90.

[28] V. Agarwal, G.W. Bell, J.-W. Nam, D.P. Bartel, Predicting effective microRNA target sites in mammalian mRNAs, Elife 4 (2015) 1–38, https://doi.org/10.7554/eLife.05005.

[29] P. Malenfant, D.R. Joanisse, R. Theriault, B.H. Goodpaster, D.E. Kelley, J.A. Simoneau, Fat content in individual muscle fibers of lean and obese subjects, Int. J. Obes. 25 (9) (2001) 1316–1321, https://doi.org/10.1038/sj.ijo.0801733.

[30] J.D. Wood, M. Enser, A.V. Fisher, G.R. Nute, P.R. Sheard, R.I. Richardson, S.I. Hughes, F.M. Whittington, Fat deposition, fatty acid composition and meat quality: a review, Meat Sci. 78 (4) (2008) 343–358, https://doi.org/10.1016/j.meatsci.2007.07.019.

[31] C. Xiao, T. Sun, Z. Yang, L. Zou, J. Deng, X. Yang, Whole-transcriptome RNA sequencing reveals the global molecular responses and circRNA/lncRNA-miRNA-mRNA ceRNA regulatory network in chicken fat deposition, Poultry Sci. 101 (11) (2022), https://doi.org/10.1016/j.psj.2022.102121.

[32] N. Bougarne, B. Weyers, S.J. Desmet, J. Deckers, D.W. Ray, B. Staels, K. De Bosscher, Molecular actions of PPARα in lipid metabolism and inflammation, Endocrine 39 (5) (2018) 760–802, https://doi.org/10.1210/er.2018-00064.

[33] J. San, Y. Du, G. Wu, R. Xu, J. Yang, J. Hu, Transcriptome analysis identifies signaling pathways related to meat quality in broiler chickens - the extracellular matrix (ECM) receptor interaction signaling pathway, Poultry Sci. 100 (6) (2021) 101135, https://doi.org/10.1016/j.psj.2021.101135.

[34] H. Gu, M. Gan, L. Wang, Y. Yang, J. Wang, L. Chen, S. Zhang, Y. Zhao, L. Niu, D. Jiang, Y. Chen, A. Jiang, L. Shen, L. Zhu, Differential expression analysis of tRNA-derived small RNAs from subcutaneous adipose tissue of obese and lean Pigs, Animals 12 (24) (2022) 3561, https://doi.org/10.3390/ani12243561.

[35] R. Davoli, S. Braglia, M. Zappaterra, C. Redeghieri, M. Comella, P. Zambonelli, Association and expression analysis of porcine ACLY gene related to growth and carcass quality traits in Italian Large White and Italian Duroc breeds, Livest. Sci. 165 (2014) 1–7, https://doi.org/10.1016/j.livsci.2014.04.010.

[36] E.M. Palsson-McDermott, L.A.J. O'Neill, Targeting immunometabolism as an anti-inflammatory strategy, Cell Res. 30 (4) (2020) 300–314, https://doi.org/10.1038/s41422-020-0291-z.

[37] K. Iizuka, K. Takao, D. Yabe, ChREBP-Mediated regulation of lipid metabolism: involvement of the gut microbiota, liver, and adipose tissue, Front. Endocrinol. 11 (2020) 587189, https://doi.org/10.3389/fendo.2020.587189.

[38] T.F. Osborne, Sterol regulatory element-binding proteins (SREBPs): key regulators of nutritional homeostasis and insulin action, J. Biol. Chem. 275 (42) (2000) 32379–32382, https://doi.org/10.1074/jbc.R000017200.

[39] A. Albuquerque, C. Ovilo, Y. Nunez, R. Benitez, A. Lopez-Garcia, F. Garcia, M.d.R. Felix, M. Laranjo, R. Charneca, J.M. Martins, Comparative transcriptomic analysis of subcutaneous adipose tissue from local pig breeds, Genes 11 (4) (2020) 422, https://doi.org/10.3390/genes11040422.

[40] M. Liu, Y. Chen, B. Huang, S. Mao, K. Cai, L. Wang, X. Yao, Tumor-suppressing effects of microRNA-612 in bladder cancer cells by targeting malic enzyme 1 expression, Int. J. Oncol. 52 (6) (2018) 1923–1933, https://doi.org/10.3892/ijo.2018.4342.
[41] J. Corominas, Y. Ramayo-Caldas, A. Puig-Oliveras, J. Estelle, A. Castello, E. Alves, R.N. Pena, M. Ballester, J.M. Folch, Analysis of porcine adipose tissue transcriptome reveals differences in de novo fatty acid synthesis in pigs with divergent muscle fatty acid composition, BMC Genom. 14 (2013) 1–14, https://doi.org/10.1186/1471-2164-14-843.
[42] R. Lahey, A.N. Carley, X. Wang, C.E. Glass, K.D. Accola, S. Silvestry, J.M. O'Donnell, E.D. Lewandowski, Enhanced redox state and efficiency of glucose oxidation with miR based suppression of maladaptive NADPH-dependent malic enzyme 1 expression in hypertrophied hearts, Circ. Res. 122 (6) (2018) 836–845, https://doi.org/10.1161/circresaha.118.312660.
[43] M. Rosario Ramirez, D. Morcuende, R. Cava, Fatty acid composition and adipogenic enzyme activity of muscle and adipose tissue, as affected by Iberian x Duroc pig genotype, Food Chem. 104 (2) (2007) 500–509, https://doi.org/10.1016/j.foodchem.2006.11.059.
[44] K. Xing, F. Zhu, L. Zhai, S. Chen, Z. Tan, Y. Sun, Z. Hou, C. Wang, Identification of genes for controlling swine adipose deposition by integrating transcriptome, whole-genome resequencing, and quantitative trait loci data, Sci. Rep. 6 (2016) 23219, https://doi.org/10.1038/srep23219.
[45] M. Sourdioux, C. Brevelet, Y. Delabrosse, M. Douaire, Association of fatty acid synthase gene and malic enzyme gene polymorphisms with fatness in turkeys, Poultry Sci. 78 (12) (1999) 1651–1657, https://doi.org/10.1093/ps/78.12.1651.
[46] L. Xiong, J. Pei, M. Chu, X. Wu, Q. Kalwar, P. Yan, X. Guo, Fat deposition in the muscle of female and male yak and the correlation of yak meat quality with fat, Animals 11 (7) (2021) 2142, https://doi.org/10.3390/ani11072142.
[47] J.Y. Hong, J.-i. Park, K. Cho, D. Gu, H. Ji, S.E. Artandi, P.D. McCrea, Shared molecular mechanisms regulate multiple catenin proteins: canonical Wnt signals and components modulate p120-catenin isoform-1 and additional p120 subfamily members, J. Cell Sci. 123 (24) (2010) 4351–4365, https://doi.org/10.1242/jcs.067199.
[48] U. Rappe, T. Schlechter, M. Aschoff, A. Hotz-Wagenblatt, I. Hofmann, Nuclear ARVCF protein binds splicing factors and contributes to the regulation of alternative splicing, J. Biol. Chem. 289 (18) (2014) 12421–12434, https://doi.org/10.1074/jbc.M113.530717.
[49] S. Mas, M. Bernardo, P. Gasso, S. Alvarez, C. Garcia-Rizo, M. Bioque, B. Kirkpatrick, A. Lafuente, A functional variant provided further evidence for the association of ARVCF with schizophrenia, Am. J. Med. Genet. B 153B (5) (2010) 1052–1059, https://doi.org/10.1002/ajmg.b.31073.
[50] E.D. Rosen, The transcriptional basis of adipocyte development, Prostaglandins Leukot, Essent Fatty Acids 73 (1) (2005) 31–34, https://doi.org/10.1016/j.plefa.2005.04.004.
[51] F. Roehrig, A. Schulze, The multifaceted roles of fatty acid synthesis in cancer, Nat. Rev. Cancer 16 (11) (2016) 732–749, https://doi.org/10.1038/nrc.2016.89.
[52] H. Liu, X. Wu, Z. Dong, Z. Luo, Z. Zhao, Y. Xu, J.-T. Zhang, Fatty acid synthase causes drug resistance by inhibiting TNF-alpha and ceramide production, J. Lipid Res. 54 (3) (2013) 776–785, https://doi.org/10.1194/jlr.M033811.
[53] L. Sheng, P.K. Jena, H.-X. Liu, Y. Hu, N. Nagar, D.N. Bronner, M.L. Settles, A.J. Baumler, Y.-J.Y. Wan, Obesity treatment by epigallocatechin-3-gallate-regulated bile acid signaling and its enriched Akkermansia muciniphila, Faseb. J. 32 (12) (2018) 6371–6384, https://doi.org/10.1096/fj.201800370R.
[54] J. Zhang, W. Wang, N. Feng, X. Jiang, S. Zhu, Y.Q. Chen, Ndufa6 regulates adipogenic differentiation via Scd1, Adipocyte 10 (1) (2021) 646–657, https://doi.org/10.1080/21623945.2021.2007590.
[55] C.F. Semenkovich, Regulation of fatty acid synthase (FAS), Prog. Lipid Res. 36 (1) (1997) 43–53, https://doi.org/10.1016/s0163-7827(97)00003-9.
[56] Z. Miao, F. Zhu, H. Zhang, X. Chang, H. Xie, J. Zhang, Z. Xu, Developmental patterns of FASN and LIPE mRNA expression in adipose tissue of growing Jinhua and Landrace gilts, Czech J. Anim. Sci. 55 (12) (2010) 557–564, https://doi.org/10.17221/2514-cjas.
[57] K. Xing, F. Zhu, L. Zhai, H. Liu, Y. Wang, Z. Wang, S. Chen, Z. Hou, C. Wang, Integration of transcriptome and whole genomic resequencing data to identify key genes affecting swine fat deposition, PLoS One 10 (4) (2015) e0122396, https://doi.org/10.1371/journal.pone.0122396.
[58] K. Xing, X. Zhao, H. Ao, S. Chen, T. Yang, Z. Tan, Y. Wang, F. Zhang, Y. Liu, H. Ni, Y. Guo, Z. Hou, C. Wang, Transcriptome analysis of miRNA and mRNA in the livers of pigs with highly diverged backfat thickness, Sci. Rep. 9 (2019) 16740, https://doi.org/10.1038/s41598-019-53377-x.
[59] A. Canovas, R. Quintanilla, M. Amills, R.N. Pena, Muscle transcriptomic profiles in pigs with divergent phenotypes for fatness traits, BMC Genom. 11 (2010) 1–15, https://doi.org/10.1186/1471-2164-11-372.
[60] Y. Qiao, Z. Huang, Q. Li, Z. Liu, C. Hao, G. Shi, R. Dai, Z. Xie, Developmental changes of the FAS and HSL mRNA expression and their effects on the content of intramuscular fat in Kazak and Xiniiang sheep, J Genet Genomics 34 (10) (2007) 909–917, https://doi.org/10.1016/s1673-8527(07)60102-7.
[61] Y.g. Wang, X.h. Qu, Y. Yang, X.g. Han, L. Wang, H. Qiao, Q.m. Fan, T.t. Tang, K.r. Dai, AMPK promotes osteogenesis and inhibits adipogenesis through AMPK-Gfil-OPN axis, Cell. Signal. 28 (9) (2016) 1270–1282, https://doi.org/10.1016/j.cellsig.2016.06.004.
[62] B. Shi, Z. Zhang, X. Lv, K. An, L. Li, Z. Xia, Screening of genes related to fat deposition of pekin ducks based on transcriptome analysis, Animals 14 (2) (2024) 268, https://doi.org/10.3390/ani14020268.
[63] A. Everard, H. Plovier, M. Rastelli, M. Van Hul, A.d.W. d'Oplinter, L. Geurts, C. Druart, S. Robine, N.M. Delzenne, G.G. Muccioli, W.M. de Vos, S. Luquet, N. Flamand, V. Di Marzo, P.D. Cani, Intestinal epithelial N-acylphosphatidylethanolamine phospholipase D links dietary fat to metabolic adaptations in obesity and steatosis, Nat. Commun. 10 (1) (2019) 457, https://doi.org/10.1038/s41467-018-08051-7.
[64] Y.K.J. Zhang, K.C. Wu, J. Liu, C.D. Klaassen, Nrf2 deficiency improves glucose tolerance in mice fed a high-fat diet, Toxicol. Appl. Pharmacol. 264 (3) (2012) 305–314, https://doi.org/10.1016/j.taap.2012.09.014.
[65] D.N. Kwon, B.S. Chang, J.H. Kim, MicroRNA dysregulation in liver and pancreas of CMP-Neu5Ac hydroxylase null mice disrupts insulin/PI3K-AKT signaling, BioMed Res. Int. 2014 (2014) 1–12, https://doi.org/10.1155/2014/236385.
[66] J. Xu, L. Zhang, G. Shu, B. Wang, microRNA-16-5p promotes 3T3-L1 adipocyte differentiation through regulating EPT1, Biochem. Biophys. Res. Commun. 514 (4) (2019) 1251–1256, https://doi.org/10.1016/j.bbrc.2019.04.179.
[67] A.S. Gasparotto, D.O. Borges, M.G.M. Sassi, A. Milani, D.L. Rech, M. Terres, P.B. Ely, M.J. Ramos, N.G. Meihnardt, V.S. Mattevi, Differential expression of miRNAs related to angiogenesis and adipogenesis in subcutaneous fat of obese and nonobese women, Mol. Biol. Rep. 46 (1) (2019) 965–973, https://doi.org/10.1007/s11033-018-4553-5.
[68] Y. He, S. Xu, Y. Qi, J. Tian, F. Xu, Long noncoding RNA SNHG25 promotes the malignancy of endometrial cancer by sponging microRNA-497-5p and increasing FASN expression, J. Ovarian Res. 14 (1) (2021) 1–13, https://doi.org/10.1186/s13048-021-00906-w.
[69] C. Wu, S. Fang, H. Zhang, X. Li, Y. Du, Y. Zhang, X. Lin, L. Wang, X. Ma, Y. Xue, M. Guan, Long noncoding RNA XIST regulates brown preadipocytes differentiation and combats high-fat diet induced obesity by targeting C/EBPα, Mol. Med. 28 (1) (2022) 1–11, https://doi.org/10.1186/s10020-022-00434-3.
[70] M.J. Hu, M. Long, R.J. Dai, Acetylation of H3K27 activated lncRNA NEAT1 and promoted hepatic lipid accumulation in non-alcoholic fatty liver disease via regulating miR-212-5p/GRIA3, Mol. Cell. Biochem. 477 (1) (2022) 191–203, https://doi.org/10.1007/s11010-021-04269-0.
[71] C. Lin, Z. Dong, J. Song, S. Wang, Y. Yang, H. Li, Z. Feng, Y. Pei, Differences in histomorphology and expression of key lipid regulated genes of four adipose tissues from Tibetan pigs, PeerJ 11 (2023) e14556, https://doi.org/10.7717/peerj.14556.
[72] Z. Yang, X. Chen, M. Yu, R. Jing, L. Bao, X. Zhao, K. Pan, B. Chao, M. Qu, Metagenomic sequencing identified microbial species in the rumen and cecum microbiome responsible for niacin treatment and related to intramuscular fat content in finishing cattle, Front. Microbiol. 15 (2024) 1334068, https://doi.org/10.3389/fmicb.2024.1334068.
[73] J. Chen, R. You, Y. Lv, H. Liu, G. Yang, Conjugated linoleic acid regulates adipocyte fatty acid binding protein expression via peroxisome proliferator-activated receptor α signaling pathway and increases intramuscular fat content, Front. Nutr. 9 (2022) 1029864, https://doi.org/10.3389/fnut.2022.1029864.
[74] W. Zhang, Y. Liao, P. Shao, Y. Yang, L. Huang, Z. Du, C. Zhang, Y. Wang, Y. Lin, J. Zhu, Integrated analysis of differently expressed microRNAs and mRNAs at different postnatal stages reveals intramuscular fat deposition regulation in goats (Capra hircus), Anim. Genet. 55 (2) (2024) 238–248, https://doi.org/10.1111/age.13384.
[75] A.V. Shinde, C. Humeres, N.G. Frangogiannis, The role of alpha-smooth muscle actin in fibroblast-mediated matrix contraction and remodeling, BBA-Mol Basis, Dissent 1863 (1) (2017) 298–309, https://doi.org/10.1016/j.bbadis.2016.11.006.

[76] M. Shao, L. Vishvanath, N.C. Busbuso, C. Hepler, B. Shan, A.X. Sharma, S. Chen, X. Yu, Y.A. An, Y. Zhu, W.L. Holland, R.K. Gupta, De novo adipocyte differentiation from Pdgfr beta(+) preadipocytes protects against pathologic visceral adipose expansion in obesity, Nat. Commun. 9 (2018) 890, https://doi.org/10.1038/s41467-018-03196-x.
[77] D. Merrick, A. Sakers, Z. Irgebay, C. Okada, C. Calvert, M.P. Morley, I. Percec, P. Seale, Identification of a mesenchymal progenitor cell hierarchy in adipose tissue, Science 364 (6438) (2019) 353–377, https://doi.org/10.1126/science.aav2501.
[78] M.V. Plikus, C.F. Guerrero-Juarez, M. Ito, Y.R. Li, P.H. Dedhia, Y. Zheng, M. Shao, D.L. Gay, R. Ramos, T.-C. Hsi, J.W. Oh, X. Wang, A. Ramirez, S.E. Konopelski, A. Elzein, A. Wang, R.J. Supapannachart, H.-L. Lee, C.H. Lim, A. Nace, A. Guo, E. Treffeisen, T. Andl, R.N. Ramirez, R. Murad, S. Offermanns, D. Metzger, P. Chambon, A.D. Widgerow, T.-L. Tuan, A. Mortazavi, R.K. Gupta, B.A. Hamilton, S.E. Millar, P. Seale, W.S. Pear, M.A. Lazar, G. Cotsarelis, Regeneration of fat cells from myofibroblasts during wound healing, Science 355 (6326) (2017) 748–752, https://doi.org/10.1126/science.aai8792.
[79] E. Sidorenko, M. Sokolova, A.P. Pennanen, S. Kyheroinen, G. Posern, R. Foisner, M.K. Vartiainen, Lamina-associated polypeptide 2 alpha is required for intranuclear MRTF-A activity, Sci. Rep. 12 (1) (2022) 2306, https://doi.org/10.1038/s41598-022-06135-5.
[80] N. Li, Q.-L. Yu, X.-M. Yan, H.-B. Li, Y. Zhang, Sequencing and characterization of miRNAs and mRNAs from the longissimus dorsi of Xinjiang brown cattle and Kazakh cattle, Gene 741 (2020) 144537, https://doi.org/10.1016/j.gene.2020.144537.
[81] C. Mai, C. Wen, C. Sun, Z. Xu, S. Chen, N. Yang, Implications of gene inheritance patterns on the heterosis of abdominal fat deposition in chickens, Genes 10 (10) (2019) 824, https://doi.org/10.3390/genes10100824. Genes 10 (10) (2019).
[82] M.A. Alam, M.M. Rahman, Mitochondrial dysfunction in obesity: potential benefit and mechanism of Co-enzyme Q10 supplementation in metabolic syndrome, J. Diabetes Metabol. 13 (1) (2014) 60–70, https://doi.org/10.1186/2251-6581-13-60.
[83] X. Zhang, C. Liu, Y. Kong, F. Li, X. Yue, Effects of intramuscular fat on meat quality and its regulation mechanism in Tan sheep, Front. Nutr. 9 (2022) 908355, https://doi.org/10.3389/fnut.2022.908355.
[84] L. Zhao, F. Li, X. Zhang, D. Zhang, X. Li, Y. Zhang, Y. Zhao, Q. Song, K. Huang, D. Xu, J. Cheng, J. Wang, W. Li, C. Lin, W. Wang, Integrative analysis of transcriptomics and proteomics of longissimus thoracis of the Hu sheep compared with the Dorper sheep, Meat Sci. 193 (2022) 108930, https://doi.org/10.1016/j.meatsci.2022.108930.
[85] H. Li, Y.H. Feng, C. Xia, Y. Chen, X.-Y. Lu, Y. Wei, L.L. Qian, M.Y. Zhu, G.Y. Gao, Y.F. Meng, Y.L. You, Q. Tian, K.Q. Liang, Y.T. Li, C.T. Lv, X.Y. Rui, M.Y. Wei, B. Zhang, Physiological and transcriptomic analysis dissects the molecular mechanism governing meat quality during postmortem aging in Hu sheep (Ovis aries), Front. Nutr. 10 (2024) 1321938, https://doi.org/10.3389/fnut.2023.1321938.
[86] A. Cederberg, L.M. Gronning, B. Ahren, K. Tasken, P. Carlsson, S. Enerback, FOXC2 is a winged helix gene that counteracts obesity, hypertriglyceridemia, and diet-induced insulin resistance, Cell 106 (5) (2001) 563–573, https://doi.org/10.1016/s0092-8674(01)00474-3.
[87] Y. Yao, M. Suraokar, B.G. Darnay, B.G. Hollier, T.E. Shaiken, T. Asano, C.-H. Chen, B.H.J. Chang, Y. Lu, G.B. Mills, D. Sarbassov, S.A. Mani, J.L. Abbruzzese, S.A. G. Reddy, BSTA promotes mTORC2-mediated phosphorylation of akt1 to suppress expression of FoxC2 and stimulate adipocyte differentiation, Sci. Signal. 6 (257) (2013) 1–25, https://doi.org/10.1126/scisignal.2003295.
[88] K.E. Davis, M. Moldes, S.R. Farmer, The forkhead transcription factor FoxC2 inhibits white adipocyte differentiation, J. Biol. Chem. 279 (41) (2004) 42453–42461, https://doi.org/10.1074/jbc.M402197200.
[89] C. Castano, S. Kalko, A. Novials, M. Parrizas, Obesity-associated exosomal miRNAs modulate glucose and lipid metabolism in mice, P Natl Acad Sci USA 115 (48) (2018) 12158–12163, https://doi.org/10.1073/pnas.1808855115.
[90] C. Shi, F. Huang, X. Gu, M. Zhang, J. Wen, X. Wang, L. You, X. Cui, C. Ji, X. Guo, Adipogenic miRNA and Meta-signature miRNAs involved in human adipocyte differentiation and obesity, Oncotarget 7 (26) (2016) 40830–40845, https://doi.org/10.18632/oncotarget.8518.
[91] Z. Yang, Z. Xiao, H. Guo, X. Fang, J. Liang, J. Zhu, J. Yang, H. Li, R. Pan, S. Yuan, W. Dong, X.-L. Zheng, S. Wu, Z. Shan, Novel role of the clustered miR-23b-3p and miR-27b-3p in enhanced expression of fibrosis-associated genes by targeting TGFBR3 in atrial fibroblasts, J. Cell Mol. Med. 23 (5) (2019) 3246–3256, https://doi.org/10.1111/jcmm.14211.
[92] Y. Hou, L. Fu, J. Li, J. Li, Y. Zhao, Y. Luan, A. Liu, H. Liu, X. Li, S. Zhao, C. Li, Transcriptome analysis of potential miRNA involved in adipogenic differentiation of C2C12 myoblasts, Lipids 53 (4) (2018) 375–386, https://doi.org/10.1002/lipd.12032.